Efficient Turbo Inter-Leaver Based MIMO-OFDM System For Low Complexity Outdoor Communication

D. Lalitha Kumari, M.N. Giri Prasad

Abstract*: *An arrangement of multiple antennas in both the receiver and transmitter called Multiple Input and Multiple Output (MIMO). The Orthogonal Frequency Division Multiplexing (OFDM) is enabled in MIMO system for high data wireless communications. Combination of both MIMO and OFDM Access (OFDMA) is a growing technology in next generation communication systems. In this work, the Bit Error Rate (BER) performance of MIMO-OFDMA is analyzed with Orthogonal Space Time Block Code (OSTBC), Maximum Ratio Combining (MRC) and Turbo coding scheme over flat fading channel are named as MIMO-MRC-OFDMA. OSTBC is a transmit diversity scheme, which is utilized for delivering an efficient transmission with high peak data rates that significantly improves the capacity of communication systems. Successively, the MRC diversity solves transmit and receive diversity from an OSTBC. MRC approach is applied in the receiving end for summing and weighing the received signals from the multiple paths. Besides, turbo coding scheme is utilized for error correction in a given code rate. The proposed system performance is evaluated in light of BER by varying the number of receive and transmit antennas such as 2×2, 2×4, 4×2 and 4×4.

Index Terms*: *MRC diversity, orthogonal frequency division multiplexing, space time block code, turbo encoding and decoding scheme.

I. INTRODUCTION

In present decades, MIMO is extensively utilized for enhancing the multipath propagation by radio link capacity multiplication in multiple transmitting and receiving antennas. The scalability and flexibility of MIMO system are selected in the next generation wireless networks. In Medium Voltage (MV) network, Narrowband Power-Line Communication (NB-PLC) application is created by the design of MIMO-OFDM [1]. The Signal-to-Noise Ratio (SNR) of ordered post processing describes the detected BER of bit-interleaved and coded MIMO-OFDM links. The post processing is established over the subcarriers [2]. So, Channel Estimation (CE) is required to avoid the channel fading in OFDM, while the coherent detection is present in the MIMO system [3]. Based shallow water model, the channel model has assumed as the MIMO with Multi-Carrier (MC) system in an underwater communication [4]. In MIMO, the degradation of CE is alleviated by the OFDM receiver and it uses the low complexity phase noise mitigation. The effect of moving user, foliage and shadowing are analyzed in an outdoor atmosphere [5-6].

Revised Manuscript Received on October 05, 2019

D. Lalitha Kumari, Department of ECE, JNTUACEA, Anantapur, India.

M.N. Giri Prasad, Department of ECE, JNTUACEA, Anantapur, India.

The special protection of Side Information (SI), and Peak to Average Power Ratio (PAPR) reduction are performed by Selected Mapping (SLM) in MIMO-OFDM [7]. The physical layer security is enhanced in MIMO-OFDM system using passive eavesdropper. The secure transmission is performed using spatial beam forming and artificial noise broadcasting [8]. In addition, a spectral Wireless Optical Broadband Access Network (WOBAN) is used in MIMO-OFDM for achieving high data rates, high capacity range and high spectral efficiency [9-10]. In alamouti coded MIMO-OFDM systems, PAPR reduction is carried out by using an adaptive clipping technique, which is used for extracting the successive peaks [11]. Based on the block matrix (BM) approach, the blind subspace CE is performed in MIMO-OFDM systems. The received OFDM symbols are grouped, which are collected by the BM scheme into a vector form [12].

In interference channel, the maximum degree is obtained by Interference Alignment (IA). For effective communication, the transmit chains corresponds to the two transmit antennas per user [13]. Wireless environment in the dynamic nature of MIMO-OFDM is developed by link adoption. The location of spatial stream is damaged by ordering the spatial streams that leads to insufficiency in subcarrier ordering [14]. In MIMO-OFDM, a corrupted failed packet is retransmitted by using OSTB system at the modulation layer. On the basis of Forward Error Correction (FEC), throughput of the system is varied [15]. The above mentioned approaches have some constraints such as high BER and inadequate data transmission. To overcome these constraints, Turbo encoder and decoder is included in MIMO-OFDMA. The Quadrature Phase Shift Keying (QPSK) modulation is used in MIMO-OFDMA system to transmit the data in a specific time period between the pair of antennas. The overall process of MIMO-OFDMA in turbo coding along with OSTBC coding are named as MIMO-MRC-OFDMA. Performance of the proposed system is enhanced by enabling Maximum Ratio Combining (MRC) diversity technique with resource allocation. Performance of the proposed system is evaluated in light of SNR and BER.

II. RELATED WORKS

Xu Chao et al. [16] presented a theory of compressed sensing in the MIMO-OFDM systems and also a low complexity pilot designing algorithm was introduced for achieving a non-orthogonal pilot pattern. In this work, the Mean Square Error (MSE) was normalized by CS channel estimation, which delivers a better outcome than the orthogonal pilot pattern. Here,

the BER and NMSE values were high that degrades the effectiveness of the desired MIMO system. Yang Dong and Tian Xinji et al. [17] developed space time code and codeword space alignment in MIMO channel to eliminate the interference, which was presented in the transmission signal. The nodes that were presented in the MIMO system accepts alamouti code and it has two process stages like Multiple Access (MA) stage and Broadcast (BC) stage. Feedback was greatly decreased and it doesn't require the Channel State Information (CSI) at BC stage. The modulation square decides the difficulty in ML decoding.

Guo Mangqing et al. [18] resolved the issue of pilot contamination in MIMO by introducing a channel estimation algorithm: Enhanced Eigenvalue Decomposition (EEVD). The relationship between the coefficient matrix of channel fast fading and covariance matrix of the received pilot signal decides the behavior of EEVD algorithm. The inter cell and intra cell intrusion was rejected by multiplying the received signal with normalized base vector-matrix conjugate transpose. Van Canh Tran et al. [19] developed a new method in Amplify-and-Forward (AF) MIMO-Spatial Division Multiplexing for resolving the signal combining in the destination and cooperative relay selection. The developed method was utilized for recovering the signal at the destination. In a few circumstances, if the amount of nodes present in the MIMO-SDM was increased that may affect the BER performances. Geng Xuan et al. [20] concentrated on linear transceiver design in MIMO Interference Channel (IC). The developed design effectively lessens the MSE with each transmitter power constraint. In this research study, MIMO achieves less computational complexity, when the system has a large amount of antennas. In contrast, the transceivers do not have the data about perfect CSI.

III. MIMO-MRC-OFDMA SYSTEM

The MIMO-MRC-OFDMA is utilized for enhancing the wireless communication channel capacity. Here, the MIMO-OFDMA system is enabled with the arrangement of turbo decoding and encoding for avoiding the burst errors in data transmission. Turbo encoder contains two Recursive Systematic Convolutional (RSC) and internal inter-leaver design, and also it comprises of de-inter-leaver for decoding the data, which is received from the OSTBC decoder. The OSTBC is used for transferring the data packets in a specific time period and also it improves the spectrum efficiency. In contrast, the reliability and SNR are improved by using MRC diversity technique along with the channel estimator. Consider the number of users for transmitting and receiving the information in an efficient manner and the information of proposed system is transmitted over the slowly varying AWGN channel. The work flow of proposed system is shown in Fig. 1.

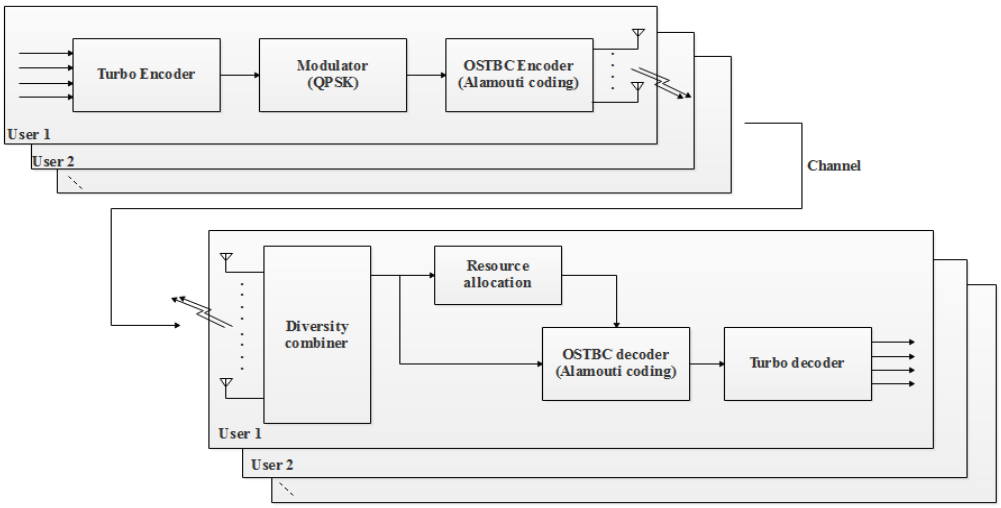

Fig. 1. Work flow of proposed system

A. MIMO-OFDM system model

There are three main parts in MIMO-OFDM system such as, transmitter *TX* , channel *h* and receiver *RX* . Where, N_T *and* N_R are denoted as amount of transmitter and receiver antennas, which are placed in the input and output. Fig. 2 shows the typical MIMO-OFDM model. MIMO-OFDM system is defined in light of channel *h* . For instance, several inputs are positioned in the transmitter output and numerous outputs are located at the input of the receiver. The channel with N_R outputs and N_T inputs are represented as a matrix of form $N_T \times N_R$, which is given in Eq. (1).

$$h = \begin{pmatrix} h_{1,1} & h_{1,2} & h_{1,1} & h_{1,N_T} \\ h_{2,1} & h_{2,2} & \cdots & h_{2,N_T} \\ \vdots & \vdots & \ddots & \vdots \\ h_{N_T,1} & h_{N_R,2} & \cdots & h_{N_R,N_T} \end{pmatrix} \quad (1)$$

Where, $h_{j,k}$ is represented as entry attenuation and phase shift (transfer function) among the k^{th} transmitter and receiver j .

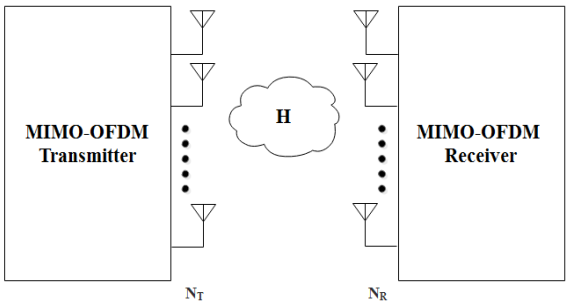

Fig. 2. Block diagram for MIMO-OFDM system

B. Turbo coding scheme

Turbo coding attains good proximate Shannon limit error correction by simple component codes and interleaver. The features of turbo coding depend on the procedure of iterative decoding, RSC encoders and interleaver. Turbo codes are used to enhance the efficiency of data transmission in MIMO-MRC-OFDMA. The upcoming operation is performed by turbo encoder, interleaver and turbo decoder, which are explained as follows.

1) Turbo encoder

Turbo encoder contains two identical RSC encoders, which is connected in parallel with an inter-leaver. RSC encoders are divided by an inter-leaver within the range of $r = 1/2$. Where, r is stated as code rate of the desired communication. The similar data are collected from two RSC encoders that is permutated by an inner inter-leaver and then transmitted to second RSC encoder. The behavior of the convolutional code is defined by two parameters: constraint length K and the code rate r . The RSC encoders should have smaller constraint length to avoid the excessive decoding complexity of the turbo encoder. Successively, the turbo encoder gives three kinds of outputs such as O^1, O^2 *and* O^3 .From the output of two RSC encoders, only one output is utilized. Though, the systematic output of one RSC encoder is a permutated version of the adopted RSC encoder. The block diagram of turbo encoder is given in Fig. 3.

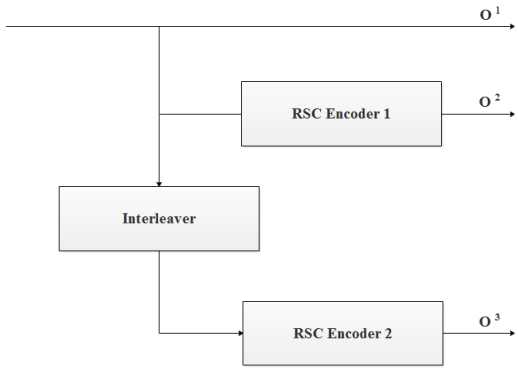

Fig. 3. Block diagram of Turbo encoder

2) Inter-leaver

Bursty error patterns are randomized in RSC encode using inner inter-leaver. In inner inter-leaver, the training data (for instance, 1) is added for every data samples, which is delivered by the turbo encoder that is graphically denoted in figure 4. Here, the noises are made the differences in data packets during the data transmission. The training data is transferred from 1 to 0 at the time of error occurs. Random noise is generated at the receiver, while performing data transmission until it achieves the errorless data packets.

w_0	1	x_0	1	y_0	1	z_0	1	. . . . .	w_4	1	x_4	1	y_4	1	z_4	1

Fig. 4. Data samples with training data

C. Modulation

In the proposed system, QPSK modulation is applied, which is a digital modulation technique. Quadrature means the signal shifts between the states of phase that are divided by 90°. The QPSK modulation increases the signal to 90° from 45° to $135^\circ, -45^\circ\left(315^\circ\right)$,or $-135^\circ\left(225^\circ\right)$. There are two channels (I and Q) are used in QPSK modulation. QPSK transfers two bits simultaneously over AWGN channel. In QPSK modulation, two carrier frequencies are identical, but the respective phase is offset by 90°. For each channel, two carriers are added and it is assigned to the respective channel modulator and the bandwidth for the modulation is two bits/second/Hz. The constellation diagram for QPSK modulation is given in Fig. 5.

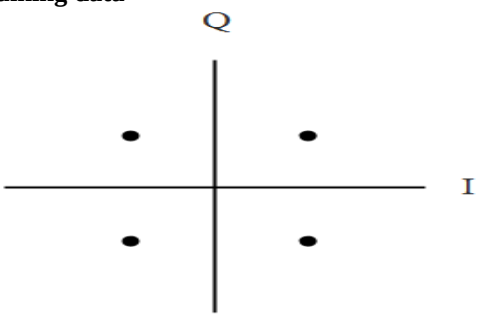

Fig. 5. Constellation diagram of QPSK modulation

D. Orthogonal space time block code scheme

After the modulation procedure, OSTBC encoder and decoder are utilized to encode and decode the data packets. OSTBC is a complex version of Alamouti's space time code, which is utilized for mapping the modulated symbols of the transmission matrix. A transmission matrix $P \times N_T$ is

consider, where P is denoted as time slot and N_T is stated as transmit antennas. The different symbol columns are delivered over the dissimilar kind of antennas and also in different time slots and symbol rows are transmitted. Besides, OSTBC decoding is attained by maximum likelihood and linear processing of the receiver. Consider an OFDM system with N amount of subcarriers, in that only active subcarriers are selected N_A. The remaining subcarriers are called virtual subcarriers that are derived from the Eq. (2).

$$N_v = N - N_A \tag{2}$$

In transmitter end, the bit streams are mapped and assembled into complex symbols. The OFDM symbols transmitted through OSTBC is mathematically denoted in Eq. (3).

$$S_j = \left[O_{Nv/2\times1} S_j^{-T} O_{NV/2\times1} \right] \tag{3}$$

Where, O is denoted as guard band, S_j is indicated as length of data vector. In first OFDM symbol period, s_1 and s_2 are transmitted from the transmit antenna. In next OFDM symbol period, s_1^* *and* s_2^* are transmitted from the antenna 1 and 2. The encoding matrix of OSTBC encoder is given in Eq. (4).

$$S = \begin{pmatrix} s_1 & s_2 \\ -s_2^{\,*} & s_1^{\,*} \end{pmatrix} \tag{4}$$

The obtained OFDM symbols are given in the Eqs. (5) and (6).

$$y_1^{\circ} = h_{1,1}s_1 + h_{2,1}s_2 + n_1 \tag{5}$$

$$y_2^{\circ} = -h_{1,1}s_2\,{}^* + h_{1,2}s_2\,{}^* + n_2 \tag{6}$$

Where, y_1° and y_2° are denoted as received $N1$ symbol period from antenna 1 and 2, $h_{\mathrm{j,k}}$ is denoted as NN transmission matrix from the k^{th} transmit antenna to the j^{th} receive antenna, n_1 *and* n_2 are indicated as $N1$ complex Gaussian random noise. After performing serial to parallel conversion, the received time domain signal is converted into frequency domain using FFT operation. Eqs. (7) and (8) indicates frequency domain signals.

$$y_1 = Fy_1^{\circ} + Fn_1^{\circ} \tag{7}$$

$$y_2 = Fy_2^{\circ} + Fn_2^{\circ} \tag{8}$$

Eq. (9) shows the symbols from the OFDM.

$$\begin{bmatrix} y_1 \\ y_2^* \end{bmatrix} = \begin{bmatrix} h_{1,1} & h_{2,1} \\ h_{2,2}^* & -h_{1,2}^* \end{bmatrix} \cdot \begin{bmatrix} s_1 \\ s_2 \end{bmatrix} + \begin{bmatrix} n_1 \\ n_2^* \end{bmatrix} \tag{9}$$

The received signal is achieved by rewriting the Eq. (9), as mentioned in the Eq. (10).

$$y = Hs + n \tag{10}$$

E. MRC diversity with resource allocation in channel

MRC diversity technique is used in AWGN channel for combining the diversity and channel estimator used in MIMO-MRC-OFDMA system. The perfect information about the received signals like phases, amplitudes and the individual signals from each branch is weighted based on their signal voltage to noise power produces the perfect combining in MRC diversity technique. MRC diversity technique is also named as perfect combining. This MRC is an optimum diversity scheme for enhancing the capacity for all combining techniques. The highest number of SNR is achieved by combining all the signals in co-phased and weighted manner. Resource allocation is used for decreasing the Co Channel Interference (CCI). This CCI is maximized when the spatial correlation is increased in the data transmission. Resource allocation is mainly depending on the three statements. Initially, it is assumed that the CSI is estimated and the feedback of CSI is send to the transmitter. Then, the CSI is accessible before starting the data transmission. Channel condition does not change when the symbol transmission block of OFDM eliminated the allocated resources by obsolete CSI. The efficient resource allocation of MIMO-MRC-OFDMA requires frequent updates of channel information [21]. The SNR is maximized, when the signals of the receiver's output are linearly combined. Consider the complex envelope of received signal of the j^{th} diversity branch as described in the following Eq. (11).

$$x(t) = \alpha_j e^{k\theta_j} \hat{s}(t) + w_j(t) \le t \le T_j = 1,2,\ldots \mathrm{N} \tag{11}$$

Where, the modulated signal complex envelope is represented as $\hat{s}(t)$, it is delivered during the symbol interval $0 \le t \le T$ for the j^{th} diversity branch, $\alpha_j e^{k\theta_j}$ denotes the fading in terms of multiplicative term and the additive white channel noise is represented as $w_j(t)$. The maximal ratio combiner of N is kept in the receiver end and it is followed by a linear combiner. The corresponding complex envelope of the linear combiner output is given in Eq. (12).

$$y(t) = \sum_{j=1}^{N} \alpha_j x_j(t) \tag{12}$$

By substituting Eq. (11) in (12), the liner combiner output is obtained and it is given in the Eq. (13).

$$y(t) = \hat{s}(t) \sum_{j=1}^{N} \alpha_j \alpha_j e^{k\theta_j} + x_j(t) + \sum_{j=1}^{N} \alpha_j w(t) \tag{13}$$

Where, the complex weighting parameters are denoted as α_j, which describes the linear combiner.

1) Effective SNR with MRC

Sum of random variables is an effective symbol energy to noise ratio. The rapid bit energy to noise ratio in j^{th} receive antenna is given in following Eq. (14).

$$\gamma = \frac{|\alpha_j|^2 E_b}{N_o}$$

(14)

The channel is equalized with the N amount of receive antenna and the adequate bit energy to noise ratio is given in the Eq. (15)

$$\gamma_{mrc} = \sum_{j=1}^{N} \frac{|\alpha_j|^2 E_b}{N_o} = N\gamma_i \quad \gamma_m \tag{15}$$

2) Error rate MRC

Sum of N random variables is the effective symbol energy to noise ratio γ_{mrc}. The SNR probability density function is given by the Eq. (16),

$$f(\gamma_{mrc}) = \frac{1}{(N-1)!} \frac{\gamma_{mrc} N - 1}{\gamma_a N} e^{\left(\frac{\gamma mrc}{\gamma a}\right)} \tag{16}$$

Where, the average SNR in the output of j^{th} receiver is denoted as γ_a.

For maximum ratio combining E_b / N_0 is interchanged by the γ_{mrc}. The instantaneous output SNR γ_{mrc} is a random variable. The average of conditional probability about γ_{mrc} determines the probability density function of γ_{mrc}, which is given in Eq. (17).

$$P_e = E\left[\Pr ob(error \vee \gamma_{mrc})\right] \tag{17}$$

The above Eq. (17) is multiplied by the conditional probability $\text{Prob}(error \vee \gamma_{mrc})$ by the PDF of γ_{mrc} and then it is incorporated as γ_{mrc}.

$$P_e = \int_0^{\infty} \Pr ob(error \mid \gamma_{rmc}) f(\gamma_{mrc}) d\gamma_{mrc} \tag{18}$$

The Eq. (18) is concluded that the P_e differs by raising γ_a to the N^{th} power. Thus with MRC, the BER minimizes inversely with the N^{th} power of the SNR.

F. Turbo decoder

Turbo decoder receives the inputs from OSTBC decoder and it is being processed. The turbo decoder contains two Maximum a Posteriori (MAP) decoders and it is separated by the inner inter-leaver that permutes the input sequence. The decoding process of turbo decoder is iterative process and the extrinsic information is shared among the MAP decoders. A single turbo iteration is separated as two half iterations. The MAP decoder 1 and MAP decoder 2 is on, when the first and second half of iteration is performed, respectively. Both the decoders create the priori information for the respective decoder. The inter-leaver of turbo decoder is similar to the inter-leaver of turbo encoder. Random noise generation is done to achieve the error free data packets. The approximate form of the original data is obtained in the output of the turbo decoder. By using the inter-leaver in the decoder, the packet loss is minimized. Because if the system causes more erroneous packets (corrupted data) while performing the data transmission, it affects the system reliability and also it affects the SNR. Figure 6 shows the block diagram of turbo decoder.

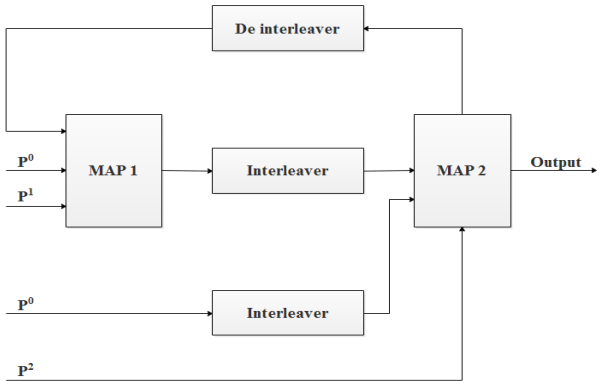

Fig. 6. Block diagram of Turbo decoder.

Turbo decoding is accomplished by two Soft Input Soft Output (SISO) component decoders. This SISO decoders exchanges the soft information (data about sub stream). The systematic information, interleaved information and the correlating parity information are sent to each decoder by BCJR (Bahl, Cocke, Jelinek and Raviv), Log-MAP algorithms. The turbo decoder calculates the extrinsic information from another decoder. Usually, a complex model system $y = (hs + n)$ is used in sphere decode, as mentioned in Eq. (19).

$$\begin{bmatrix} R(y) \\ I(Y) \end{bmatrix} = \begin{bmatrix} R(h) & -I(h) \\ I(h) & R(h) \end{bmatrix} + \begin{bmatrix} R(n) \\ I(n) \end{bmatrix} \tag{19}$$

Where, the real and imaginary parts of the variables are denoted as R *and* I respectively.

1) Maximum a posteriori probability (MAP) detection in SISO

The optimal MAP algorithms are used in this SISO MIMO detection. The exact posteriori probability of each bit is determined by 2^{QM} possible symbol combinations of MAP algorithm. Log-Likelihood Ratio (LLR) expresses the probability of MAP algorithms. Binary decision about the corresponding bit is determined by LLR value sign, when the LLR magnitude specifies the decision reliability. The j^{th} symbol LLR of the c^{th} bit is computed by using Eq. (20).

$$L(x_{j,c}) = \log \frac{P(x_{j,c} = +1 \vee y)}{P(x_{j,c} = -1 \vee y)} = \log \frac{\sum_{s \in \chi_{j,c}^{+1}} p(y \vee s) p(s)}{\sum_{s \in \chi_{j,c}^{-1}} p(y \vee s) p(s)} \tag{20}$$

Where, the sets of symbol vectors corresponding to the j^{th} symbol and having the c^{th} bit of symbol equal to +1 and -1(representing a logical 1 and a logical 0) are represented as a $\chi_{j,c}^{+1}$ *and* $\chi_{j,c}^{-1}$ respectively. The conditional probability density function $p(y \vee s)$ is given in the Eq. (21).

$$p(y \mid s) = \frac{1}{(\pi N_o)} e^{\left(\frac{-1}{N_o}\|y - hs\|^2\right)}$$

(21)

The channel decoder provides the priori information $P(s)$ as given in Eq. (23) and this information of priori LLRs is in Eq. (22).

$$L_A\left(x_{j,c}\right)=\log\frac{P\left(x_{j,c}=+1\right)}{P\left(x_{j,c}=+1\right)},\forall j,c \tag{22}$$

$$P(s)=\prod_{j=1}^{M}P\left(s_j\right)=\prod_{j=1}^{M}\prod_{c=1}^{Q}P\left(x_{j,c}\right) \tag{23}$$

Max-Log-Map approximation calculates the LLR values from Eq. (24) for reducing the computational complexity.

$$L\left(x_{j,c}\right)\approx\frac{1}{N_0}\min_{\chi_{j,c}^{-1}}\{d_1\}-\frac{1}{N_o}\min_{\chi_{j,c}^{+1}}\{d_1\} \tag{24}$$

Where, the Euclidean distance among the collected vector y and to the lattice points hs is represented as d_1 that is given in the following Eq. (25).

$$d_1=\|y-hs\|^2-N_o\log\left(P(s)\right)$$

$$\|y-hs\|^2-N_o\sum_{j=1}^{M}\sum_{c=1}^{Q}\log P\left(x_{j,c}\right) \tag{25}$$

Depends on a posteriori LLRs $L\left(x_{j,c}\right)$ and a priori LLRs, $L_A\left(x_{j,c}\right)$ the extrinsic LLRs are calculated by the detector, it is expressed in Eq. (26).

$$L_E\left(x_{j,c}\right)=L\left(x_{j,c}\right)-L_A\left(x_{j,c}\right) \tag{26}$$

The LLR computation employs MAP detection used with low-order modulations and a less number of antennas. Because, the system complexity maximizes exponentially by the amount of transmit antennas and orders of modulation.

IV. RESULTS AND DISCUSSION

In this research work, MIMO-MRC-OFDMA system is evaluated using MATLAB 2017b tool with communication (for the simulation purpose) i5 desktop computing environment with 8 GB RAM memory capacity. The MIMO-MRC-OFDMA system consists of MRC with turbo coding scheme in OSTBC.

Table I. Simulation parameters

MIMO-MRC-OFDMA system testing	
Data bits	50000 bits data's (with pocket size of 25)
Sampling rate	1e6
Path delays	0 to 2e-6
Path gain	0 to -10
Modulation & demodulation	QPSK
Channel encoding & decoding	OSTBC
Data Encoding	Turbo coding
Channel type	AWGN with Rayleigh fading (Fast flat fading)
Antenna type	2 × 2, 2 × 4, 4 × 2 and 4 × 4
SNR value for analysis	-35:10:45

The MIMO-MRC-OFDMA system is tested based on the parameters as mentioned in table 1. There are 50000 random bits are developed (with the sampling rate of 2e-6 and block size of 25). After generating the random bits, which are transferred to the turbo encoding process. In turbo encoder, the interleaver bits are generated based on data frame size. If the data has 50000 bits in the encoding process, the interleaver generates 50000 interleaved bits. These interleaved bits are used in the turbo encoding process and then the turbo encoder produces 750048 bits based on the both 50000 data bits and 50000 interleaved bits. After generating the interleaved bits (750048 bits), QPSK modulation modulates the bits and it gives the output of 375024 bits. The modulator output is in the form of 50×1 and the CP is combined in the next step. Data are generated in the form of $0.4\times$ length (mod Data (375024 bits)) and the generated CP is 150009 bits. By using CP, IFFT is carried out which gives the output of 525033 bits.

Data transferred to the OSTBC is changed that depends on the amount of receiver antennas used in OSTBC receiver. For example, if the input of encoder data is 525033×1, the encoded data of OSTBC is in 70044×4 for four receiver antennas. In case the receiver antenna is 2, the output of OSTBC is 70044×2. The antenna design is utilized in the transmissions like 2×2, 4×2 and 4×4. AWGN with Rayleigh fading are added in the transmitted signal by propagating the signal in the AWGN with Rayleigh fading environment. Combination of AWGN with Rayleigh fading is named as fast flat fading. The problem caused by the fast flat fading is overcome by combining the method with an interleaving between the coding process. From the analysis, MRC is a superior combining technique, which provide effective interleaving in combination with turbo coding scheme. So, the turbo encoder is used with the maximum ratio combining technique. Here, the noise is added based on the SNR value (-35:10:45).

In receiving section, the antennas such as 2×2, 2×4, 4×2 and 4×4 receives the signal, which are affected by noise. In addition, the MRC diversity is utilized in OSTBC encoder for combining the signals in co-phased and weighted manner that generates 700044×4 or 700044×2 bits, which depends on the receiver antenna. The output of MRC is transmitted to the OSTBC decoder, which generates the output of 525033×1. These bits are performing FFT process to produce the output in the form of 375024 bits. The demodulation of QPSK is performed in the received FFT signals and it delivers 750048 bits. These bits are decoded by using the turbo decoder. From the received signal of turbo decoder (50000 bits), the BER and the error rate are analyzed.

In MIMO-MRC-OFDMA system, the transmission among the various users are analyzed and the developed system has × number of transmitting and receiving antennas for all users. From this analysis, the performance between the numerous users is analyzed. Each user has inner data transmission with some degradation and improvement in the uplink and downlink. The performance of single user is analyzed and it is compared with Equal Gain Combining (EGC) systems by

means of BER. The Different number of transmitter and receiver antennas are used such as 2×2, 2×4, 4×2 and 4×4 for analyzing the BER value.

Table II. Analysis of BER for 2×2 MIMO-MRC-OFDMA system

SNR	-35	-25	-15	-5	5	15	25	35
EGC	0.00491	0.004883	0.004906	0.004934	0.004906	0.004969	0.004653	0.004028
MIMO-MRC-OFDMA	0.004886	0.005034	0.004905	0.004994	0.004879	0.004776	0.004061	0.000256

Table 2 and figure 7 states the comparison of 2×2 MIMO-MRC-OFDMA with EGC system. From the performance study, it is concluded that the MIMO-MRC-OFDMA gives better enhancement in SNR.

Table III. Analysis of BER for 2×4 MIMO-MRC-OFDMA system

SNR	-35	-25	-15	-5	5	15	25	35
EGC	0.000497	0.000493	0.000495	0.000489	0.000496	0.000486	0.000477	0.000387
MIMO-MRC-OFDMA	0.0005	0.000487	0.000495	0.000492	0.000489	0.000473	0.000369	0.000361

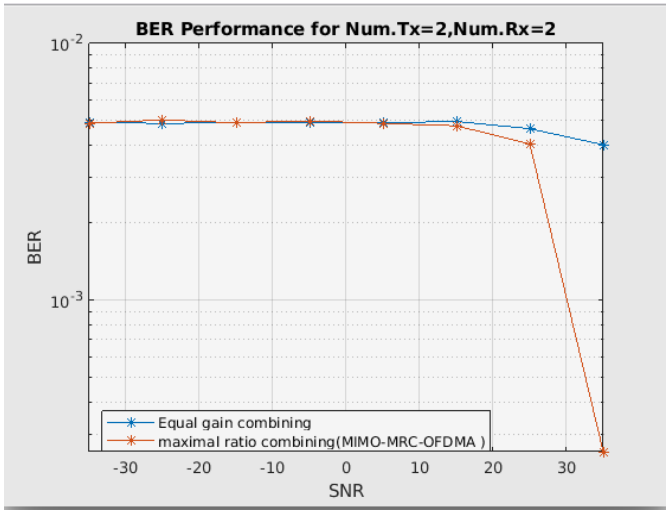

Fig. 7. BER analysis for 2×2 MIMO-MRC-OFDMA system

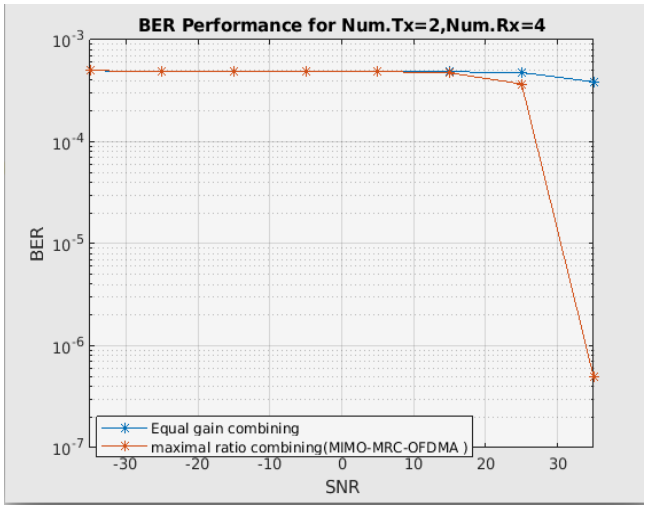

Fig. 8. BER analysis for 2×4 MIMO-MRC-OFDMA system

The performance of 2×4 MIMO-MRC-OFDMA is analyzed with EGC system in table 3 and figure 8. From table 3, it is concluding that the MIMO-MRC-OFDMA has less BER than the EGC algorithm.

Table IV. Analysis of BER for 4×4 MIMO-MRC-OFDMA system

SNR	-35	-25	-15	-5	5	15	25	35
EGC $\times10^{-5}$	4.9725	4.96	4.94625	4.89625	4.8425	4.8775	4.64875	3.00375
MIMO-MRC-OFDMA $\times10^{-5}$	5.04125	4.95625	4.95375	4.99625	4.83625	4.44625	2.38375	1.32375

Table 4 and figure 9 shows the performance analysis of 4×4 MIMO-MRC-OFDMA system. The performance study showed that the MIMO-MRC-OFDMA has better SNR and a small amount of BER than the EGC

Table V. Analysis of BER for 4×2 MIMO-MRC-OFDMA system

SNR	-35	-25	-15	-5	5	15	25	35
EGC	0.000496	0.000496	0.000488	0.0005	0.000494	0.000487	0.000455	0.000322
MIMO-MRC-OFDMA	0.000494	0.000493	0.000488	0.000489	0.000487	0.000463	0.000343	0.000291

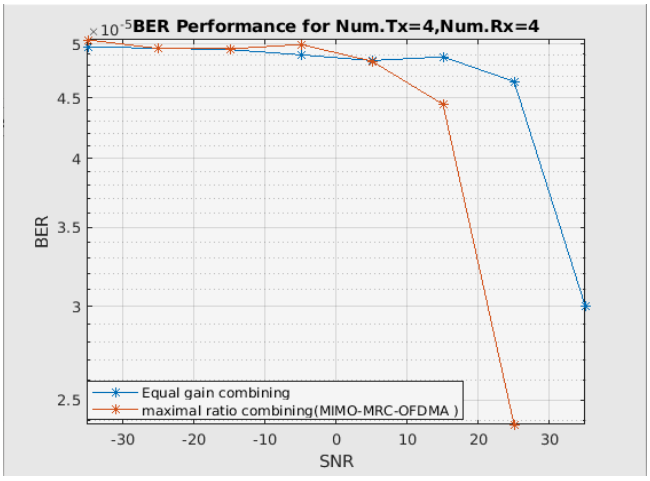

Fig. 9. BER analysis for 4 × 4 MIMO-MRC-OFDMA system

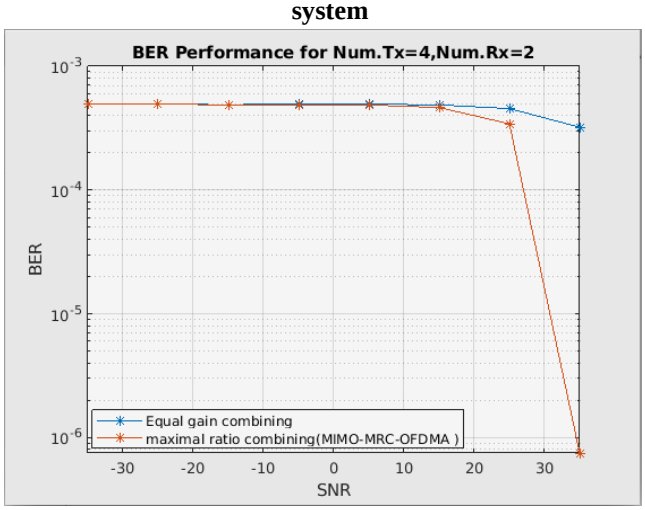

Fig. 10. BER analysis for 2 × 4 MIMO-MRC-OFDMA system. BER analysis for 42 MIMO-MRC-OFDMA system

Table 5 and figure 10 shows the performance study of 4 × 2 MIMO-MRC-OFDMA system. The error rate performance of the 4 × 2 MIMO-MRC-OFDMA is improved by decreasing the BER value, because the MIMO-MRC-OFDMA has MRC diversity combiner at the input of OSTBC decoder that improves the performance of the desired system.

V. CONCLUSION

The proposed system comprises of MIMO-OFDMA with orthogonal space time block code, MRC diversity technique and turbo encoding and decoding. Initially, the data are encoded in the turbo encoder, then the encoded data bits are modulated under QPSK modulation. Turbo encoding and decoding schemes are employed with the interleaver to obtain approximate Shannon limit error correction among the data transmission. The diversity technique of MRC is utilized at the input of OSTBC decoder for combining the signals in weighted and co-phased manner. In the experimental phase, the proposed system performance is analyzed by varying the amount of transmit and receive antennas such as 2 × 2, 2 × 4, 4 × 2 and 4 × 4. From the experimental analysis, the proposed system averagely reduced 0.01-0.05 error rate related to the existing system. The proposed system has less bit error rate than the EGC system. In the future, an effective coding scheme is developed for further improving the BER in MIMO-OFDMA.

REFERENCES

1. A. I. Chrysochos, T. A. Papadopoulos, A. ElSamadouny, G.K. Papagiannis, and N. Al-Dhahir. (2016). Optimized MIMO-OFDM design for narrowband-PLC applications in medium-voltage smart distribution grids. *Electric Power Systems Research, 140*, pp.253-262.
2. R. C. Daniels, and W. H. Robert (2011). Modeling ordered subcarrier SNR in MIMO-OFDM wireless links. *Physical Communication 4(4)*, pp. 275-285.
3. S. Gulomjon, Y. Fu, and S. Jamshid. (2015). Optimization on semi-blind channel estimation for MIMO-OFDM systems. *The Journal of China Universities of Posts and Telecommunications, 22(6)*, pp. 86-93.
4. N. Iruthayanathan, K. S. Vishvaksenan, V. Rajendran, and S. Mohankumar. (2015). Performance analysis of turbo-coded MIMO–OFDM system for underwater communication. *Computers & Electrical Engineering, 43*, pp.1-8.
5. A. Ishaque, and G. Ascheid. (2013). Efficient MAP-based estimation and compensation of phase noise in MIMO-OFDM receivers. *AEU-International Journal of Electronics and Communications 67(12)*, pp. 1096-1106.
6. J. S. Sandeep, and B. Vidhyacharan, (2012). Performance analysis of MIMO–OFDM in various outdoor fading environments. *AEU-International Journal of Electronics and Communications 66(10)*, pp. 797-805.
7. B. M. Lee, and R. Figueiredo. (2010). MIMO-OFDM PAPR reduction by selected mapping using side information power allocation. *Digital Signal Processing 20(2)*, pp. 462-471.
8. N. Romero-Zurita, M. Ghogho, and D. McLernon. (2011). Physical layer security of MIMO–OFDM systems by beamforming and artificial noise generation. *Physical Communication, 4(4)*, pp. 313-321.
9. R. Q. Shaddad, A. B. Mohammad, and A. M. Al-Hetar. Spectral efficient hybrid wireless optical broadband access network (WOBAN) based on transmission of wireless *MIMO OFDM signals over WDM PON. Optics Communications 285(20)*, pp. 4059-4067.
10. V. Sharma, and H. Kaur. (2016). On BER evaluation of MIMO-OFDM incorporated wireless system. *Optik-International Journal for Light and Electron Optics 127(1)*, pp. 203-205.
11. S. Singh, and A. Kumar. (2016) Performance Analysis of Adaptive Clipping Technique for Reduction of PAPR in Alamouti Coded MIMO-OFDM Systems. *Procedia Computer Science, 93*, pp. 609-616.
12. J. L. Yu, B. Zhang, and C. Po-Ting. (2014) Blind and semi-blind channel estimation with fast convergence for MIMO-OFDM systems. *Signal Processing 95*, pp. 1-9.
13. O. El Ayach, S. W. Peters, and R. W. Heath. (2010). The feasibility of interference alignment over measured MIMO-OFDM channels. *IEEE Transactions on Vehicular Technology 59(9)*, pp. 4309-4321.
14. R. C. Daniels, C. M. Caramanis, and R. W. Heath. (2010). Adaptation in convolutionally coded MIMO-OFDM wireless systems through supervised learning and SNR ordering. *IEEE Transactions on vehicular Technology, 59(1)*, pp. 114-126.
15. M. Zia, I. ul Haq, N. Bhatti, and H. Mahmood. (2015). Selective chase combining for OSTB coded MIMO-OFDM system. *AEU-International Journal of Electronics and Communications, 69(5)*, pp.861-866.
16. X. Chao, Z. Jianhua, and Y. Changchuan. (2016). Non-orthogonal pilot pattern for sparse channel estimation in large-scale MIMO-OFDM system. *The Journal of China Universities of Posts and Telecommunications 23(4)*, pp. 63-68.
17. Y. Dong, and T. Xinji. (2016). Interference cancellation method based on space-time code for MIMO interference channel. *The Journal of China Universities of Posts and Telecommunications 23(3)*, pp. 45-50.
18. G. Mangqing, X. Gang, G. Jinchun, and L. Yuan'an (2015). Enhanced EVD based channel estimation and pilot decontamination for Massive MIMO networks. *The Journal of China Universities of Posts and Telecommunications, 22(6)*, pp. 72-77.
19. V. C. Tran, M. T. Le, X. N. Tran, and T. Q. Duong, (2015). MIMO cooperative communication network design with relay selection and CSI feedback. *AEU-International Journal of Electronics and Communications, 69(7)*, pp. 1018-1024.
20. G. Xuan, C. Li, and L. Feng. (2016). Low complexity robust

linear transceiver design for MIMO interference channel. *The Journal of China Universities of Posts and Telecommunications 23(6),* pp. 76-81.
21. R. O. Afolabi, A. Dadlani, and K. Kim. (2013). Multicast scheduling and resource allocation algorithms for OFDMA-based systems: A survey. IEEE Communications Surveys & Tutorials 15(1), pp. 240-254.

AUTHORS PROFILE

Mrs. D. Lalitha Kumari received her B.Tech in ECE in 2003.She has completed her Master of technology in Digital Systems And Computer Electronics in 2008..Her research interest includes wireless communication, video signal processing and digital image processing.

Dr. M.N. Giri Prasad has been completed his PhD in 2003. He has completed is Master of Technology in Electronics & Communication Eng. in 1994, and Bachelor of Engineering in 1982. His research interest includes video signal processing and digital image processing and Biomedical Signal Processing